

## A long-term controlled drug-delivery with anionic beta cyclodextrin complex in layer-by-layer coating for percutaneous implants devices

Beatriz S. Verza<sup>a</sup>, Jeroen J.J.P. van den Beucken<sup>b</sup>, João V. Brandt<sup>c</sup>, Miguel Jafelicci Junior<sup>c</sup>, Valentim A.R. Barão<sup>d</sup>, Rodolfo D. Piazza<sup>c</sup>, Oya Tagit<sup>e</sup>, Denise M.P. Spolidorio<sup>f</sup>, Carlos Eduardo Vergani<sup>a</sup>, Erica D. de Avila<sup>a,\*</sup>

<sup>a</sup> Department of Dental Materials and Prosthodontics, School of Dentistry at Araraquara, São Paulo State University (UNESP), Humaita, 1680 Araraquara, São Paulo, Brazil

<sup>b</sup> Regenerative Biomaterials, Radboudumc, Philips Van Leydenlaan 25, Nijmegen, the Netherlands

<sup>c</sup> Department of Physical Chemistry, Institute of Chemistry, São Paulo State University (UNESP), Araraquara, São Paulo 14801-970, Brazil

<sup>d</sup> Department of Prosthodontics and Periodontology, Piracicaba Dental School, University of Campinas (UNICAMP), Av. Limeira, 901, Piracicaba, São Paulo 13414-903, Brazil

<sup>e</sup> Department of Tumor Immunology, Radboudumc and Radboud Institute for Molecular Life Sciences (RIMLS), Geert Grooteplein Zuid, 28 Nijmegen, the Netherlands

<sup>f</sup> Department of Physiology and Pathology, School of Dentistry at Araraquara, São Paulo State University (UNESP), Araraquara, São Paulo 14801-903, Brazil

### ARTICLE INFO

#### Keywords:

Drug delivery  
Cyclodextrin  
Layer-By-Layer  
Percutaneous device  
Coating

### ABSTRACT

This study demonstrated a drug-delivery system with anionic beta cyclodextrin ( $\beta$ -CD) complexes to retain tetracycline (TC) and control its release from multilayers of poly(acrylic acid) (PAA) and poly(L-lysine) (PLL) in a ten double layers ([PAA/PLL]<sub>10</sub>) coating onto titanium. The drug-delivery capacity of the multilayer system was proven by controlled drug release over 15 days and sustained released over 30 days. Qualitative images confirmed TC retention within the layer-by-layer (LbL) over 30 days of incubation. Antibacterial activity of TC/anionic  $\beta$ -CD released from the LbL was established against *Staphylococcus aureus* species. Remarkably, [PAA/PLL]<sub>10</sub>/TC/anionic  $\beta$ -CD antibacterial effect was sustained even after 30 days of incubation. The non-cytotoxic effect of the multilayer system revealed normal human gingival fibroblast growth. It is expected that this novel approach and the chemical concept to improve drug incorporation into the multilayer system will open up possibilities to make the drug release system more applicable to implantable percutaneous devices.

### 1. Introduction

Among implant categories, percutaneous devices (PDs) are synthetic materials that, comparable to a tooth, disclose one part extruding through the epithelial tissue access to the body's internal environment (Abdallah, Badran, Ciobanu, Hamdan, & Tamimi, 2017; Puckett, Lee, Ciombor, Aaron, & Webster, 2010). Ideally, the tissue surrounding the PDs should inhibit apical epithelial migration and provide a biological seal between the material and soft tissues to protect the implant against mechanical forces and microorganisms. However, the fact that the oral mucosa/skin-implant interface does not totally isolate the internal environment may facilitate pathogen invasion into the body (Abdallah et al., 2017; Groeger & Meyle, 2015; Peramo & Marcelo, 2010).

Microbial infection act as a prelude to mechanical disruption of the tissue/implant interface with loss of implant function (Stacy et al., 2014). Beside loss of implants, the dreaded infection around PDs may have harmful consequences to general health, causing significant morbidity, mortality, and generating considerable healthcare costs (Affeld, Grosshauser, Goubergrits, & Kertzscher, 2012; Campoccia, Montanaro, & Arciola, 2006; Puckett et al., 2010). It was estimated that in the United States only, a total of 82,000 deaths annually are caused by medical device-related infections, with a huge financial burden of \$18 billion on healthcare services (Xu et al., 2017). Among PDs, the exposed pins or wires, as a necessary component of the modern orthopedic surgery, are related to the most common orthopedic infections that may arise from percutaneous pins or wires. The susceptibility of pin sites to

\* Corresponding author.

E-mail addresses: [beatriz.verza@hotmail.com](mailto:beatriz.verza@hotmail.com) (B.S. Verza), [jeroen.vandenbeucken@radboudumc.nl](mailto:jeroen.vandenbeucken@radboudumc.nl) (J.J.J.P. van den Beucken), [joao.brandt@gmail.com](mailto:joao.brandt@gmail.com) (J.V. Brandt), [miguel.jafelicci@unesp.br](mailto:miguel.jafelicci@unesp.br) (M. Jafelicci Junior), [vbarao@unicamp.br](mailto:vbarao@unicamp.br) (V.A.R. Barão), [rodolfo.piazza@gmail.com](mailto:rodolfo.piazza@gmail.com) (R.D. Piazza), [oyatagit@gmail.com](mailto:oyatagit@gmail.com) (O. Tagit), [denise.mp.spolidorio@unesp.br](mailto:denise.mp.spolidorio@unesp.br) (D.M.P. Spolidorio), [carlos.vergani@unesp.br](mailto:carlos.vergani@unesp.br) (C.E. Vergani), [erica.fobusp@yahoo.com.br](mailto:erica.fobusp@yahoo.com.br) (E.D. de Avila).

<https://doi.org/10.1016/j.carbpol.2020.117604>

Received 17 October 2020; Received in revised form 22 December 2020; Accepted 30 December 2020

Available online 5 January 2021

0144-8617/© 2021 Elsevier Ltd. All rights reserved.

infection occurs when the skin barrier is disrupted. The percentage of patients suffering from orthopedic device-related infections is significant. In the past, infection rates around PDs were >50 % for external fixators (Mahan, Seligson, Henry, Hynes, & Dobbins, 1991). More recently, data from the Center of Orthopedic Osseointegration in Gothenburg revealed that approximately 38 % of osseointegrated arm prostheses were infected within five years of implantation, and 17 % failed (Tsikandylakis, Berlin, & Branemark, 2014). In case of dental implants, the prevalence of infection, known as peri-implantitis, rate range from 16 to 48% during an observation period of 9–14 years (Koldstrand, Scheie, & Aass, 2010). During oral infection disease progress, a high number of pathogenic bacteria from the infected oral site can gain access into the bloodstream and reach vital organs, such as lungs, heart, and peripheral blood capillary system (Han & Wang, 2013; Li, Kolltveit, Tronstad, & Olsen, 2000; Scannapieco & Mylotte, 1996). The fact that key oral microbial species might be associated with systemic diseases such as cancer, rheumatoid arthritis, diabetes, and some other severe chronic diseases, has increased the impact of oral pathologic conditions on general health (Kane, 2017).

Over the past years, with the appropriate surgical procedures involving aseptic environment and techniques, and adequate prophylactic systemic antibiotic applied as standard protocols, the incidence of infections associated to PD implants has decreased (Abdallah et al., 2017; Yue et al., 2015). Still, infections of implanted devices represent one of the most serious and devastating medical complications (Affeld et al., 2012; Hollenbeak & Schilling, 2018; Percival, Suleman, Vuotto, & Donelli, 2015; Zimlichman et al., 2013). To date, despite disease complexity and increased knowledge about the action mechanisms involved in disease initiation that allow a range of directions to halt disease progression (Beline et al., 2019; Costa et al., 2020; Dini et al., 2020; Nagay et al., 2019; Souza et al., 2020), no effective management has been achieved (Yue et al., 2015). In an attempt to counteract bacterial colonization, prophylactic systemic antibiotic administration has become the standard in clinics over recent decades (Jepsen & Jepsen, 2016; Yue et al., 2015). However, the overuse and misuse of systemic antibiotic bring forward the need for new strategies to address antimicrobial resistance. Since, antibiotics still remain the major character drug used to treat infectious diseases, the potential benefit of local administration may be a preferred route to ensure its rapid onset of action and to minimize drug toxicity (Boehler et al., 2017; Reinbold et al., 2017).

Controlled release technology is an interesting and promising method for antimicrobial agent delivery to specific sites, optimization of their dose and sustainability during the release period, hence making effective and safe use of available antibiotics. In view of biomaterial devices, layer-by-layer (LbL) assembly of drug-releasing coatings represents a universal technology (de Avila, van Oirschot, & van den Beucken, 2020; Donath, Sukhorukov, Caruso, Davis, & Mohwald, 1998; Jia & Li, 2019; Stadler, Chandrawati, Goldie, & Caruso, 2009; van den Beucken et al., 2006). The abundance of available coating components and the understanding about driving forces for drug release, enable the engineering of drug-releasing coatings with a wide range of tunable properties. We recently developed a novel LbL drug-releasing coating through the sequential deposition of anionic (PAA) and cationic polyelectrolytes (PLL) via electrostatic interactions in a ten double layers ([PAA/PLL]<sub>10</sub>) coating onto titanium (Ti) (de Avila E.D. et al., 2019). This drug-releasing coating showed a burst release for tetracycline (TC) (Han & Ulevitch, 2005) within 24 h, which effectively killed *Porphyromonas gingivalis* (de Avila E.D. et al., 2019). To overcome this, we are now in a position to deepen and improve the method for drug incorporation into the multilayers to control the initial drug concentration released over time. To this end, we proposed to use the amphiphilic molecule beta-cyclodextrin ( $\beta$ -CD) to retain TC within the LbL coating and control its release from [PAA/PLL]<sub>10</sub> coatings deposited on Ti discs.  $\beta$ -CD has been proposed as a candidate molecule to improve drug loading and release owing to the cyclic oligosaccharide structure with a

relatively hydrophobic central cavity and hydrophilic outer surface (Radu, Parteni, & Ochiuz, 2016). Via this structure,  $\beta$ -CD can increase the aqueous solubility of poorly water-soluble drugs and their bioavailability and stability within a drug-releasing system (Archontaki, Vertzoni, & Athanassiou-Malaki, 2002; Arima, Miyaji, Irie, Hirayama, & Uekama, 1998, 2001; Gomez-Galvan et al., 2016). The idea of using carrier molecules of antimicrobial substances to form host-guest inclusion complexes with a variety of drugs has received increasing attention in the last years as a biomaterial-based approach for infection prevention (Drago et al., 2014). Indeed, affinity interactions between carrier molecules and drug moieties, has been proposed as a crucial property for controlling drug loading and release. Since most drugs are hydrophilic, as TC, we hypothesize that  $\beta$ -CD can be tethered into LbL for improved and coordinated release (Hasanzadeh et al., 2016; Tiwari, Tiwari, & Rai, 2010). In this study, we are following the experiments with TC as our drug of choice due to the convenient advantage of intrinsic auto-fluorescence that enables drug visualization within the LbL coating via fluorescence microscopy over time (Cha, Lee, & Kim, 2019; Jeong, Song, Cooper, Jung, & Greaves, 2010).

Here, the pathogenic bacteria species *Staphylococcus aureus* (*S. aureus*) was used to confirm the antibacterial effect of a novel LbL coating using  $\beta$ -CD for improvement of TC loading and release. Further experiments were performed to determine the efficiency of drug release in neutral (7.4) and acidic (4.5) pH conditions, since characteristics of biological environments often differ upon an inflammatory process, and these variations can have significant impact on the effectiveness of physiologically stimuli triggered release and consequently on the drug concentration available to fight disease. In addition, we investigated the extended effect of drug retained within the LbL coating up to 30 days incubation under both pH conditions.

## 2. Materials and methods

### 2.1. Materials and reagents preparation

Commercially pure titanium (Ti; Grade 2 as per the American Society for Testing Materials), machined discs (12 mm in diameter, 1.5 mm thickness) were purchased from Machinefabriek G Janssen B.V. (Valkenswaard, the Netherlands). Polyethylenimine (PEI) (m.w. = 25,000), PLL (m.w. = 15,000–30,000), tetracycline hydrochloride, UltraPure™ Tris buffer ( $\geq 99.9$  %) and sodium acetate (m.w. = 82.03),  $\beta$ -CD, epichlorohydrin (EP), chloroacetic acid (CAA) were purchased from Sigma-Aldrich (St. Louis, MO, USA). Poly(acrylic acid) (PAA; m.w. = 60,000) and sodium chloride for analysis were obtained from Polysciences (Warrington, PA, USA) and Millipore Corporation (Burlington, MA, USA), respectively.

### 2.2. Synthesis of anionic $\beta$ -CD

Anionic  $\beta$ -CD was synthesized by a one-step condensation reaction, as described by Gómez-Galván et al. (2016) (Gomez-Galvan et al., 2016). In this work, the molar ratio of the reactants was  $\beta$ -CD/EP/CAA = 1/10/2. Briefly,  $\beta$ -CD was dissolved in a NaOH 22 %w/w solution and left stirring at 25 °C for 24 h. In sequence, CAA was added to the solution and stirred. The mixture was heated to 30 °C and then EP was added quickly (600 rpm). After 3.5 h, the reaction was stopped by the addition of acetone. Acetone was posteriorly removed by decantation and the solution was neutralized with HCl. The solution was kept mixing at 50 °C overnight. After cooling, the solution was dialyzed for 4 days with a dialysis membrane of molecular weight cut-off of 3500 Da to remove unreacted EP and CAA. After dialysis, the aqueous solution was evaporated and the solid triturated with acetone. The white product was isolated by filtration and dried under vacuum (Fig. 1 and Fig. 1S).

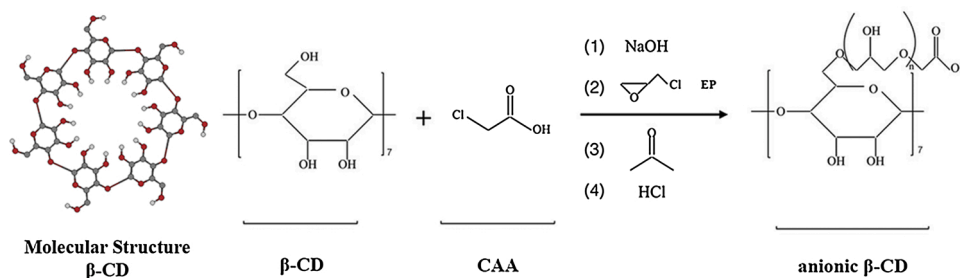


**Fig. 1.** Schematic drawing illustrating the anionic beta cyclodextrin ( $\beta$ -CD) preparation by organic addition reaction involving the functional groups of the chloroacetic acid (CAA) and epichlorohydrin (EP) molecules.

### 2.3. Preparation of TC/anionic $\beta$ -CD

The formation of inclusion complexes was performed by a co-precipitation method. The molar ratio of TC to anionic  $\beta$ -CD used was 1:1, as described by Gómez-Galván et al. (2016) (Gomez-Galvan et al., 2016). TC was stirred in 10 mL of water whereas anionic  $\beta$ -CD was dissolved in 20 mL of water at 60 °C. The resulting anionic  $\beta$ -CD solution was added to the TC solution dropwise and heated at 60 °C for 1 h and then stirred overnight at room temperature. TC/anionic  $\beta$ -CD solution was turbid and precipitation was observed subsequent to stirring overnight, indicating that TC forms an inclusion complex with anionic  $\beta$ -CD. The resulting complexes were filtered, washed with ultrapure water for three times (5000 rpm, at 25 °C for 5 min) to remove uncomplexed anionic  $\beta$ -CD and the solid TC/anionic  $\beta$ -CD was kept overnight under freezing and immediately place in the lyophilizer for 24 h, for drying.

### 2.4. TC incorporation efficiency

TC uptake by anionic  $\beta$ -CD occurred by a co-precipitation method from molar ratio of TC to anionic  $\beta$ -CD used being 1:1 (Gomez-Galvan et al., 2016). The filtered and vacuum dried TC/anionic  $\beta$ -CD was dissolved in Milli-Q water at room temperature. Sonication was used to promote fast dispersion of TC/anionic  $\beta$ -CD in water, according to the following settings: pulse on/off of 3 s, processing times of 20 min, and 21 % amplitude. TC/anionic  $\beta$ -CD sample tubes were kept in an ice bath during homogenization to avoid heating from sonication. The concentration of TC incorporated in anionic  $\beta$ -CD was determined by UV/vis spectroscopy. The TC UV-vis spectrum and analytical curve obtained at 367 nm are shown in Fig. 2S. The incorporation efficiency (IE) and incorporation coefficient (IC) percentage were calculated by the equations (1) and (2) (Deng et al., 2014):

$$IE (\%) = 1 - (W_{\text{incorporated TC}} / W_{\text{initial TC}}) \times 100 \quad (1)$$

$$IC (\%) = (W_{\text{incorporated TC}} / W_{\text{incorporated TC}} + W_{\text{anionic } \beta\text{-CD}}) \times 100 \quad (2)$$

where,  $W_{\text{incorporated TC}}$  is the total amount of TC incorporated into the anionic  $\beta$ -CD,  $W_{\text{initial TC}}$  the quantity of TC added initially during preparation, and  $W_{\text{anionic } \beta\text{-CD}}$  is the amount of anionic  $\beta$ -CD after freeze-drying.

In order to confirm the incorporation of TC into  $\beta$ -CD, fourier-transform infrared spectroscopy (FTIR) and potential zeta analyses were performed. First, FTIR measurements were obtained from TC/anionic  $\beta$ -CD by a Perkin Elmer Dual Frontier (PerkinElmer, Waltham, MA, USA) equipped with an attenuated total reflection (ATR) apparatus (zinc selenide crystal), at a resolution set of 4  $\text{cm}^{-1}$  and 128 scans per spectrum. In sequence, zeta potential values of TC/anionic  $\beta$ -CD were measured in a Zetasizer Nano series from Malvern Instruments (Nano ZS, Malvern, UK). The samples were dispersed in phosphate buffered saline (PBS) solution (pH = 7.4) at 25 °C. TC and anionic  $\beta$ -CD were used as controls. The experiments were performed in triplicate.

### 2.5. Characterization of anionic $\beta$ -CD

Nuclear magnetic resonance spectroscopy (NMR; Bruker, Bremen, Germany) was used to determine the structure of the organic compounds. Assignments for signals from  $^1\text{H}$  and  $^{13}\text{C}$  in the NMR spectra 1 mM of  $\beta$ -CD and anionic  $\beta$ -CD dissolved in deuterated solvent  $\text{D}_2\text{O}$  was recorded using a spectrometer Bruker Avance operated at 600 MHz and 25 °C.

### 2.6. Minimum bactericidal concentration determination for TC and TC/anionic $\beta$ -CD

*S. aureus* ATCC 25,923 was initially grown aerobically on Mueller Hinton (MH) agar and kept under aerobic conditions for 2 days at 37 °C. Seven bacterial colonies were transferred to MH broth medium and incubated for 18 h at 37 °C. In sequence, 500  $\mu\text{L}$  from this culture was transferred to a new tube contained 9.5 mL of fresh MH broth medium

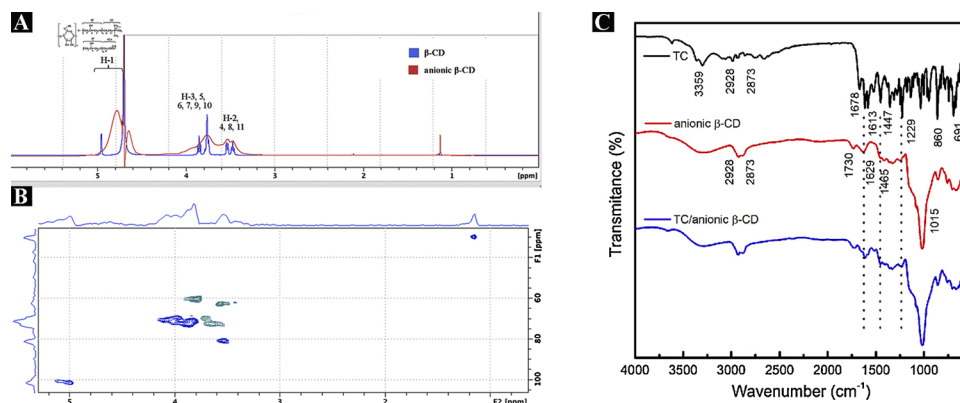


**Fig. 2.** (A)  $^1\text{H}$  NMR spectra of  $\beta$ -CD 1 mM, anionic  $\beta$ -CD 1 mM in  $\text{D}_2\text{O}$ . (B)  $^1\text{H}$  NMR and  $^{13}\text{C}$  NMR bidimensional spectra of anionic  $\beta$ -CD in  $\text{D}_2\text{O}$ . (C). FTIR spectra in the region of 3359-1678  $\text{cm}^{-1}$  to TC, 2928-2873  $\text{cm}^{-1}$ , 1730 and 1015  $\text{cm}^{-1}$  to anionic  $\beta$ -CD and, 1611-1215  $\text{cm}^{-1}$  and 1447-860  $\text{cm}^{-1}$  to TC/ anionic  $\beta$ -CD.

and kept for 4 h under aerobic incubation. *S. aureus* bacteria were adjusted to  $OD_{600nm} = 0.597$ , which correspond to  $1 \times 10^7$  colony forming units-CFU/mL, and inoculated into 96-well microliter plates (Corning Costar cell culture plates; Fisher Scientific, NY, USA) to a final bacterial density of  $10^5$  CFU/mL containing two-fold serial dilution of each drug in broth culture medium. The cultures were incubated at 37 °C under aerobic conditions, and the absorbance at  $OD_{600nm}$  read after 24 h. The lowest concentrations of TC and TC/anionic  $\beta$ -CD that inhibit *S. aureus* growth were plated and the number of viable bacteria, after 48 h of incubation, determined the minimal bactericidal concentration (MBC). MBC represented our reference concentration to calculate the amount of antibiotic to be incorporated into [PAA/PLL]<sub>10</sub> coating. *S. aureus* at the same sampling concentration were inoculated with anionic  $\beta$ -CD and directly onto polystyrene well plate to serve as our experimental controls. The experiment was performed in triplicate and repeated two times to ensure the reproducibility and reliability of data, with the exception of the experiment, in which *S. aureus* were inoculated with anionic  $\beta$ -CD. This experiment was performed in duplicate but repeated twice as technical repetition.

## 2.7. Preparation of TC/anionic $\beta$ -CD complexes-loaded [PAA/PLL]<sub>10</sub> coatings

Prior to LbL coating assembly, Ti discs were ultrasonically cleaned with acetone for 15 min, followed by a wash-step with Milli-Q water for 15 min in ultrasound, and 2-propanol for 10 min. Samples were then air-dried at room temperature for 24 h. To change the surface from hydrophobic to hydrophilic and, thus, improve the interaction between Ti and PEI, Ti discs were kept under UV-light exposure from a laminar flow hood for 20 min. In sequence, LbL coatings were assembled using the LbL assembly method as previously described (de Avila E.D. et al., 2019). Multilayered coatings were built-up by electrostatic interaction alternating PAA (1 mg/mL in a 150 mM sodium chloride solution; pH = 5.5), PLL (1 mg/mL in 10 mM of tris buffer containing 150 mM of sodium chloride; pH = 7.4) and immersion steps (each 10 min) with intermediate washing steps in Milli-Q water (1 min) to reach a [PAA/PLL]<sub>10</sub> system. As described in our previous work (de Avila E.D. et al., 2019), a ten-double layer system was mandatory to homogeneously cover the surface of Ti discs. Since TC is extremely sensitive to air and light, TC/anionic  $\beta$ -CD was prepared immediately before each experiment. Briefly, 5 mg/mL of TC/anionic  $\beta$ -CD solution was prepared in Milli-Q water at room temperature in sonicator, as described above (see section 2.4). Then, 100  $\mu$ L of TC/anionic  $\beta$ -CD at 5 mg/mL was gently dropped on the last layer, after PLL deposition being completed, and samples were statically incubated at 37 °C, in dark environment. Since coating conformation changes at 37 °C, we kept samples under established temperature for 7 days to enhance drug diffusion through the multilayered LbL (de Avila E.D. et al., 2019). In an attempt to validate the effect of anionic  $\beta$ -CD on efficiency of TC incorporation under multilayers, 100  $\mu$ L of TC at 5 mg/mL was pipetted on the last layer of PLL deposition for comparison.

## 2.8. TC/anionic $\beta$ -CD behavior onto LbL coating topography

In order to investigate the TC/anionic  $\beta$ -CD behavior on the LbL topography and to determine the surface profile, atomic force microscope (AFM) images were obtained with a Catalyst BioScope (Bruker, Bremen, Germany) coupled to a confocal microscope (TCS SP5II, Leica, Mannheim, Germany) in peak-force tapping mode using silicon nitride cantilevers with nominal spring constant of 0.7 N/m (Bruker, Bremen, Germany). At least 10 different regions of  $2 \times 2$  mm scan area were analyzed using NanoScope analysis software (Bruker, Bremen, Germany) to determine root mean squared roughness values both in air and in wet (ultrapure water) environments. For comparison, [PAA/PLL]<sub>10</sub>/TC and [PAA/PLL]<sub>10</sub> coating Ti discs were used as experimental controls.

## 2.9. Drug release and retention from the LbL coating

### 2.9.1. Standard solutions, and system suitability preparation for drug release

Three samples of each ([PAA/PLL]<sub>10</sub>/TC and [PAA/PLL]<sub>10</sub>/TC/anionic  $\beta$ -CD coating Ti discs were placed in a 50 mL tube containing 2 mL of PBS (pH = 7.4), acetate buffer (pH = 4.5) and MH culture medium (pH = 7.2), and kept at 37 °C under shaking (60 rpm/min). TC released from the coating was monitored for 1, 3, 7, 15, and 30 days. At different sampling intervals, 1 mL of supernatant was collected for analysis and a fresh solution was added into each experimental well. [PAA/PLL]<sub>10</sub> coating on Ti and uncoated Ti discs were used as controls. To determine the method detection limit, TC and TC/anionic  $\beta$ -CD standard solutions were prepared in PBS, acetate buffers and MH culture medium in the concentration range between 0.5 and 250  $\mu$ g/mL. The PBS, acetate and MH supernatant containing released TC and TC/anionic  $\beta$ -CD were analyzed by high-performance liquid chromatography machine (HPLC; Hitachi, Mannheim, Germany) consisting of a pump (Hitachi L-2130), a UV detector (Hitachi L-2400), an autosampler (Hitachi L-2200), and a LiChrospher RP-18 endcapped HPLC column (125Å~4 mm, particle size 5  $\mu$ m). The flow rate of mobile phase (formic acid buffer 0.1 % V/V and acetonitrile 90/10 vol ratio) was fixed at 0.8 mL/min with an injection volume of 30  $\mu$ L.

### 2.9.2. Drug retention within the LbL coating

The fluorescent characteristic of TC enables its visualization into the LbL system during experimental samples immersed in neutral and acidic solutions over time. TC and TC/anionic  $\beta$ -CD coating Ti discs were maintained in neutral (PBS), acidic (acetate buffer) and MH culture medium solution for 1, 3, 7, 15, and 30 days, following the same time points for drug release detection. After each period, the fluorescence intensity of the TC was analyzed by confocal laser scanning microscope (CLSM), acquiring digital images in the green channel of a CLSM (Zeiss LSM 800, Jena, Germany) with an excitation wavelength of 405 nm. Three random regions of each [PAA/PLL]<sub>10</sub>/TC and [PAA/PLL]<sub>10</sub>/TC/anionic  $\beta$ -CD coated Ti discs were acquired through 20 $\times$  Plan NeoFluar NA 0.3 air/dry and 63 $\times$  oil immersion objectives. Representative images of fluorescence staining through a 20 $\times$  objective lens were used for 3D reconstruction.

## 2.10. Biological experiments

For all biological experiments, Ti discs were sterilized in an autoclave at 121 °C for 15 min and all experimental solutions were filtered with a Millipore® membrane 0.22- $\mu$ m-pore size filters before proceeding with LbL assembly. LbL sample preparation was performed inside a biosafety cabinet.

### 2.10.1. Antibacterial activity test from as-prepared and aged samples

For this study, as-prepared samples were defined as [PAA/PLL]<sub>10</sub>/TC/anionic  $\beta$ -CD coating Ti discs immediately used after preparation. Aged samples were defined as [PAA/PLL]<sub>10</sub>/TC/anionic  $\beta$ -CD coating Ti discs kept immersed in neutral (PBS) and acidic (acetate buffer) conditions for 30 days to investigate whether the remainder of drug from the LbL coating still would have antibacterial properties. Thus, as-prepared and aged samples were placed in a 24-well culture plate (Corning Costar cell culture plates; Fisher Scientific, NY, USA) and incubated with 1 mL of *S. aureus*, in the working density ( $OD_{600nm} = 0.597$ ) under aerobic conditions. After 24 h, PBS-washed samples were transferred to a new plate containing the correspondent broth medium and bacterial cells were harvested from the discs by scraping with a pipette tip. Two hundred  $\mu$ L of bacterial culture was transferred to a 96-well plate to serial dilution procedure. Ten  $\mu$ L of each sampling well was dropped on a fresh brain heart infusion (BHI) blood agar plate and kept at 37 °C under aerobic conditions. Viable colonies were counted after 48 h. [PAA/PLL]<sub>10</sub>/TC, [PAA/PLL]<sub>10</sub> coating on Ti and uncoated Ti discs were used



as controls. Concomitantly, *S. aureus* samples at the same sampling concentration were inoculated directly onto polystyrene well plate to serve as our positive control.

### 2.10.2. Cytotoxicity assay

Human gingival fibroblast (HGF) cells (Rio de Janeiro Cell Bank Code 0089) were cultured in Dulbecco's Low Glucose Modified Eagles Medium (DMEM, Sigma Chemical Co., St. Louis, MO, USA) supplemented with 10 % fetal bovine serum (FBS, Gibco, Grand Island, NY, USA), 100 IU/mL penicillin, 100 mg/mL streptomycin (Sigma-Aldrich, St. Louis, MO, USA), and 2 mM L-glutamine (Gibco, Grand Island, NY, USA), in a humidified atmosphere containing 5% CO<sub>2</sub> at 37 °C. After reaching 90 % confluence, cells between passages 3 and 8 were washed with PBS, recovered with accutase solution (Sigma-Aldrich, St. Louis, MO), and resuspended in fresh medium. HGF cells were seeded directly onto [PAA/PLL]<sub>10</sub> coated and uncoated Ti discs at a concentration of 1 × 10<sup>5</sup> cells/well containing 5 μM carboxyfluorescein diacetate succinimidyl ester (CFSE-Cell Proliferation Kit, Life Technology, CA) and kept in an incubator with 5% CO<sub>2</sub> at 37 °C for 24 h. In order to prove the safety of drug concentrations released from [PAA/PLL]<sub>10</sub> coating Ti discs, TC/anionic β-CD at 1 mg/mL, 500 μg/mL, 100 μg/mL and 50 μg/mL was incubated in a 96-well culture plate with HGF cells at a concentration of 8 × 10<sup>3</sup> cells/well containing 5 μM carboxyfluorescein diacetate succinimidyl ester (CFSE-Cell Proliferation Kit, Life Technology, CA) in an incubator with 5% CO<sub>2</sub> at 37 °C, for 24 h. TC/anionic β-CD concentrations chose were based on the maximum of drug released concentration recorded by HPLC analyses. Fifteen minutes prior to confocal analyses, 20 μM propidium iodide (PI-LIVE/DEAD BacLight™ Bacterial Viability staining kit, Invitrogen, Carlsbad, CA, USA) was added into each well to stain dead cells. Samples were visualized with a PASCAL LSM5 confocal laser-scanning microscope (Zeiss, Jena, Germany) and images were acquired through 10 and 40× dry (Plan Neofluar NA 0.3 air) objective lens. Excitation wavelengths of 488 – 530 nm (Ar laser) and 575 – 610 nm (HeNe laser) were employed as fluorescent indicator of live (green color), and dead (red color) cells. HFG cells at the same sampling concentration were inoculated directly onto polystyrene well plates to serve as positive controls (C<sup>+</sup>). Concomitantly, cells inoculated directly onto polystyrene well plates with 9% of triton for 5 min served as death controls (C<sup>-</sup>). The experiment was performed in duplicate.

### 2.11. Statistical analysis

D'Agostino & Pearson methods were employed to test data distributions for normality. Based on the normal and homoscedastic distribution of data, statistical comparisons were performed by one-way analysis of variance (ANOVA) with a Tukey's Post Hoc test, using GraphPad Prism version 5.0c (GraphPad Software, CA, USA). All data are plotted as the mean ± standard deviation (SD) and p < 0.05 was considered statistically significant.

## 3. Results and discussion

### 3.1. Characterization of anionic β-CD

We developed a novel and simple tool for improving TC loading and release from LbL coatings for percutaneous devices. The generated [PAA/PLL]<sub>10</sub> is a well-characterized LbL coating for Ti surfaces, with remarkable features already explored, including tunable release properties, as previously shown by our research group (de Avila E.D. et al., 2019). Here, we reproduced [PAA/PLL]<sub>10</sub> coatings due to the excellent interaction between these polyelectrolytes and Ti surface, and reasoned that the coating properties would offer a mechanism to incorporate TC/anionic β-CD complex and local delivery to the implant site at biologically relevant concentrations in acidic environment. TC is a well-established bacteriostatic antibiotic, which displays

broad-spectrum activity against both Gram-positive and Gram-negative bacterial species (van den Beucken et al., 2006; de Avila E.D. et al., 2019). TC actions inhibit bacterial protein synthesis and human tissue collagenase activity, thus making it effective as a drug choice for local delivery (Cha et al., 2019; Jeong et al., 2010). Although, the dissemination of TC-resistant mechanisms has narrowed drug prescription, it is important to emphasize that the main reason for its choice in this study was the intrinsic TC autofluorescence (Stone, Butler, Phetsang, Cooper, & Blaskovich, 2018). The advantage of TC autofluorescence property enables drug visualization within the LbL coating via fluorescence microscopy to gain insight into drug release kinetics over time. In addition, drug local administration acts as a strategy to arrest the rise of antibiotic resistance since allows drug application to the site of infection at a concentration that cannot be reached by the systemic route. However, due to the hydrophilicity of TC and its weak interaction with PAA and PLL polyelectrolytes causing high TC bulk release within 24 h, we combined TC with anionic β-CD to increase both the drug loading capacity and control over drug release. CDs are cyclic oligosaccharides disclosing a hydrophobic inner cavity, which provides an apolar matrix, with a hydrophilic hydroxyl group outer surface (Gomez-Galvan et al., 2016; Laza-Knoerr, Gref, & Couvreur, 2010). The amphiphilic properties of CD allow its interaction with a wide range of molecules like ions, protein, and oligonucleotides to form inclusion complexes (Perez-Alvarez et al., 2017; Santos, Ribeiro, & Esteso, 2019; Varan, Varan, Erdoglar, Hincal, & Bilensoy, 2017). Here, we synthesized the anionic β-CD type and hypothesized that the negative charge from β-CD would sustain the deposition of TC into the [PAA/PLL]<sub>10</sub> coating, and hence would offer control over TC release.

Anionic β-CD was previously synthesized and characterized (Gomez-Galvan et al., 2016). The interacting groups involved in anionic β-CD synthesis were investigated by NMR technique. Herein, <sup>1</sup>H NMR spectra of β-CD and anionic β-CD were recorded in deuterated solvent and compared as illustrated in Fig. 2.

From interpreting the <sup>1</sup>H 1D spectrum, there is 1 chloroacetic acid moiety per glucose ring attached to the molecule. Based on that integration, the epichlorohydrin was not reactive. The heteronuclear multiple bond correlation (HMBC) to the <sup>13</sup>C and 177 ppm indicates that chloroacetic is present in the molecule identified by C=O chemical shift (Fig. 2A-B). These results indicate that negative charge from anionic molecules is incorporated into the hydrophilic group protruding from the wider opening of the β-CD.

### 3.2. TC incorporation efficiency in anionic β-CD

The succeeded incorporation of TC into anionic β-CD was demonstrated by FTIR spectroscopy with peaks characteristic of each compound being seen to increase in intensity with each respective adsorption stage (Fig. 2C). The individual adsorbed compounds have been used to provide unambiguous determination of the adsorbed mass of the TC/anionic β-CD at each stage of formation. The main signals from amide groups present in TC were observed at 3359 cm<sup>-1</sup> and 1678 cm<sup>-1</sup>, which corresponds to N-H and CO= stretching from primary amide, respectively. The signals of NH— bending of amide or amine moieties is observed at 1613 cm<sup>-1</sup> to 1519 cm<sup>-1</sup>, since both groups are present at TC structure. The CN— stretching of tertiary amine corresponds to 1229 cm<sup>-1</sup> band. The asymmetric and symmetric stretching of C-H is observed at 2928 cm<sup>-1</sup> and 2873 cm<sup>-1</sup>. The bending absorption of methylene and methyl groups are observed at 1452 cm<sup>-1</sup> and 1309 cm<sup>-1</sup>. The bands from aromatic moieties can be assigned by out of plane bending of =CH— signals at 860 cm<sup>-1</sup> and 691 cm<sup>-1</sup>, since the absorption of C=C on ring stretching (1650–1556 cm<sup>-1</sup>) could be overlapped by N-H bending. Besides the CH— stretching, the spectrum of anionic β-CD sample shows an intense band at 1015 cm<sup>-1</sup>, which is assigned as the C—OC— stretching from glucose units. The overtone bending of methylene groups (CH—) corresponds to small absorption bands around 1465 cm<sup>-1</sup>. The signal at 1730 cm<sup>-1</sup> corresponds to

carboxylic acid modification structure of  $\beta$ -CD. The spectrum of TC/anionic  $\beta$ -CD sample showed high similarity with anionic  $\beta$ -CD. The incorporation of TC is confirmed by slight shifts of interactions between TC and anionic  $\beta$ -CD, signal relative to hydrogen bonds as well as hydrophobic interactions, such as from the aromatic ring. The doublet at  $1611\text{ cm}^{-1}$  and the band at  $1215\text{ cm}^{-1}$  had their positions shifted, while the signals at  $1447\text{ cm}^{-1}$  and  $860\text{ cm}^{-1}$  had an increased intensity suggesting the incorporation of the drug (Pavia, Lampman, & Kriz, 2001).

We next performed zeta potential measurements of the surface charge of the TC/anionic  $\beta$ -CD sample. The results also suggest the TC incorporation into anionic  $\beta$ -CD, since TC surface features were preserved even after drug incorporation. Dispersed in PBS solution, the blanked anionic  $\beta$ -CD sample showed a zeta potential of  $-7.83 \pm 0.27\text{ mV}$ , which negative value is assigned to deprotonated carboxylic groups from the modification of  $\beta$ -CD. After the TC incorporation, it was observed that zeta potential presented the same magnitude ( $-7.40 \pm 0.72\text{ mV}$ ). According to Croitoru et al., TC discloses three ionizable groups, being amino group protonated in pH below 9.4 (Croitoru, Roata, Pascu, & Stanciu, 2020). In that manner, a positive zeta potential value is expected if TC is located at the outer surface of anionic  $\beta$ -CD. Thus, FTIR and zeta potential outcomes suggest that TC finds in the inner cavity of the  $\beta$ -CD, without altering the surface characteristics of the carrier.

The proportion between TC and anionic  $\beta$ -CD in terms of molar ratio was 1:1, which means that 1 g of TC was mixed with 2.27 g of anionic  $\beta$ -CD. The initial concentration of drug played a significant role in determining the drug incorporation efficiency (IE), thus the IE was evaluated from 1 mg/mL of TC. The successful TC incorporation in anionic  $\beta$ -CD was confirmed by TC values achieving at least 97 % incorporation efficiency (Fig. 3), which means that almost 100 % of the drug was incorporated by the target molecules. The high efficiency evidenced that the incorporation process depends mainly on the hydrophobic segment of the anionic  $\beta$ -CD.

### 3.3. [PAA/PLL]<sub>10</sub>/TC/anionic $\beta$ -CD coating profile in air and wet environment

In the next part of this study, the incorporation of TC/anionic  $\beta$ -CD in [PAA/PLL]<sub>10</sub> coating on Ti discs was achieved by complex diffusion into the interior of the multilayers after the last layer of PLL deposition. For comparison, [PAA/PLL]<sub>10</sub> and [PAA/PLL]<sub>10</sub>/TC were generated under the same conditions (Fig. 4). Topographical analysis in air environment

revealed significantly decreased values of roughness from [PAA/PLL]<sub>10</sub>/TC/anionic  $\beta$ -CD in contrast to [PAA/PLL]<sub>10</sub> and [PAA/PLL]<sub>10</sub>/TC, suggesting that the incorporation of TC/anionic  $\beta$ -CD macromolecules smoothens the surface. In our previous work (de Avila E.D. et al., 2019), we demonstrated that [PAA/PLL]<sub>10</sub> molecular conformation changes upon immersion in ultrapure water and displays a swelling behavior of the polyelectrolyte matrix. Our outcomes here were categorical in showing that, when samples were kept in wet condition, [PAA/PLL]<sub>10</sub>/TC/anionic  $\beta$ -CD coating Ti discs displayed the highest roughness, which indicates that LbL conformation changes and the TC/anionic  $\beta$ -CD diffusion process through the multilayered coating can contribute to increased surface irregularity, and hence roughness of the coating.

### 3.4. TC/anionic $\beta$ -CD release and retention in the LbL system

Here, we aimed to provide antimicrobial capacity within [PAA/PLL]<sub>10</sub> coating Ti discs through the incorporation of TC/anionic  $\beta$ -CD complex. Initially, [PAA/PLL]<sub>10</sub> coatings were loaded with 5 mg/mL of TC/anionic  $\beta$ -CD and then, the complex release was quantified over a period up to 30 days. For this, [PAA/PLL]<sub>10</sub>/TC/anionic  $\beta$ -CD coated Ti discs were incubated in PBS, acetate buffer and *S. aureus* culture medium (MH) to get a better understanding regarding the kinetics of drug release in different pH conditions. At each time point, 1 mL of the supernatant was collected and drug concentration determined by HPLC. [PAA/PLL]<sub>10</sub>/TC coating Ti discs were used as controls. A concentration of 62.5  $\mu\text{g/mL}$  served as our limit value to establish the minimum bactericidal concentration of TC/anionic  $\beta$ -CD to *S. aureus* (Fig. 5 - yellow arrow). Our data showed that a 10 times higher concentration of TC/anionic  $\beta$ -CD was necessary to kill 100 % of *S. aureus*, in contrast to TC (Fig. 5 - red arrow). Interestingly, a substantial *S. aureus* growth was observed when anionic  $\beta$ -CD was inoculated with bacteria in the same final density of  $1 \times 10^5\text{ CFU/mL}$ . This can be explained because cyclodextrins contain six, seven or eight glucose monomers (Kang et al., 2019; Paczkowska et al., 2019), a common sugar known for promoting *S. aureus* biofilm growth *in vitro* (Lade et al., 2019; Regassa, Novick, & Betley, 1992).

Our outcomes demonstrated that a burst release of TC/anionic  $\beta$ -CD from [PAA/PLL]<sub>10</sub> took place within the first 3 days post-incubation, independent of the incubation medium pH (Fig. 6), but conveniently occurred more pronounced in acidic pH, simulating an inflammatory process, and MH culture medium solution. Interestingly, a constant release of TC/anionic  $\beta$ -CD was observed over the first 7 days of

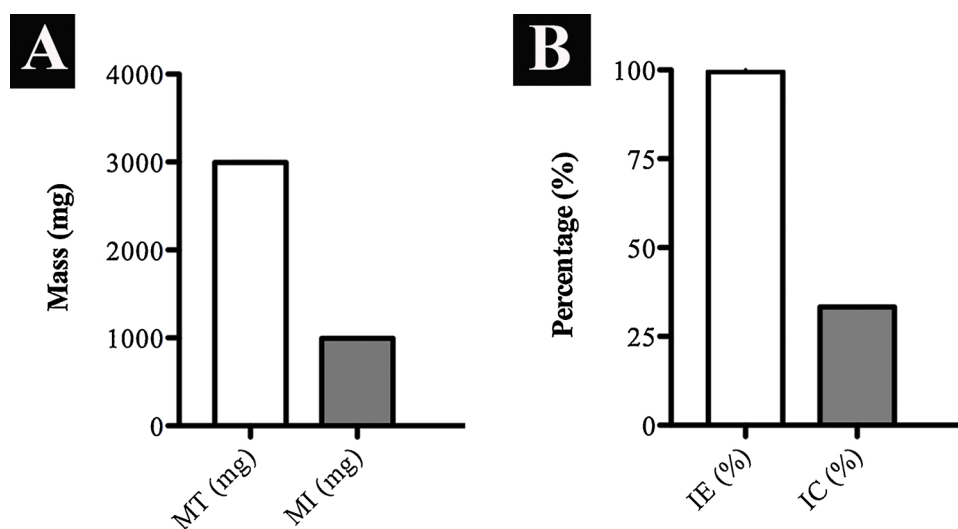


Fig. 3. (A) Total tetracycline mass (MT- white bar) and total TC mass incorporated in anionic  $\beta$ -CD (MI- light gray bar). (B) Percentage levels of incorporation efficiency (IE- white bar) and incorporation coefficient (IC- light gray bar) of TC in the anionic  $\beta$ -CD.

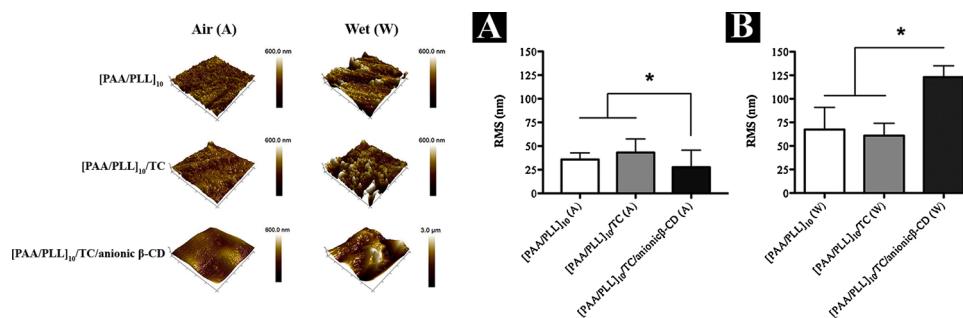


Fig. 4. AFM analyses showing TC/anionic  $\beta$ -CD effect on [PAA/PLL]<sub>10</sub> coating topography. Scan size  $10 \times 10$  nm. Effect of (A) air, and (B) wet environments on root mean square roughness of [PAA/PLL]<sub>10</sub>/TC/anionic  $\beta$ -CD (black bar) in comparison to [PAA/PLL]<sub>10</sub>/TC (gray bar - control) and [PAA/PLL]<sub>10</sub> (white bar - control) coating Ti discs. Data are shown as mean  $\pm$  standard deviation. Statistically significant differences are indicated as: \* $p < 0.0001$ .

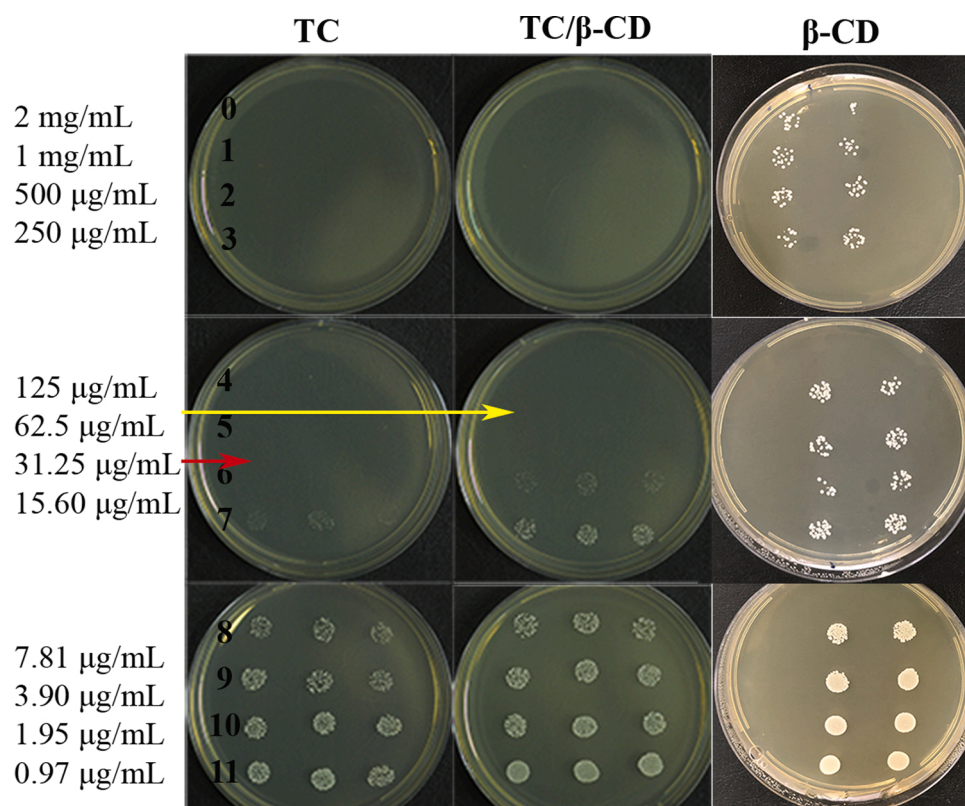


Fig. 5. *S. aureus* ATCC 25,923 bacterial growth in different concentrations of TC, TC/anionic  $\beta$ -CD, and  $\beta$ -CD, diluted 1:2 from 2 mg/mL, dilution 0, to 0.97  $\mu$ g/mL, dilution 11. Numbers from 0 to 11 refer to each dilution. Minimum bacterial concentration was recorded as a lowest drug concentration killing 100 % of the *S. aureus*: 31.25  $\mu$ g/mL (red arrow) and 62.5  $\mu$ g/mL (yellow arrow) to TC and TC/anionic  $\beta$ -CD, respectively.

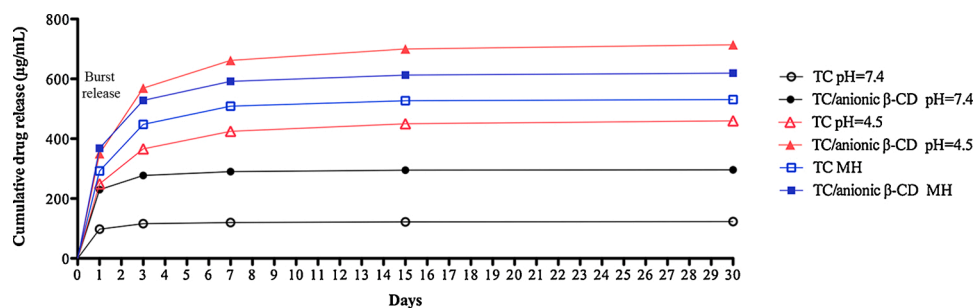


Fig. 6. The cumulative release profile of TC/anionic  $\beta$ -CD and TC in PBS (pH = 7.4), acetate buffer (pH = 4.5) and Mueller Hinton (MH) (pH = 7.2) solution at 37  $^{\circ}$ C.



incubation, with 93 and 64  $\mu\text{g}/\text{mL}$ , respectively, of the TC/anionic  $\beta$ -CD released between 3 and 7 days. After this, a relatively steady and low release of TC/anionic  $\beta$ -CD was observed between 15- and 30-days incubation. A similar outcome regarding the extended drug release time after CD interaction with the target drug was also found after 20 days (Yin et al., 2017). By contrast, previous work has reported that succeed hydrophobic and electrostatic interactions between triclosan and CD into the multilayers of polyacrylonitrile offered a burst release of drug within the first 24 h (Perez-Alvarez et al., 2017). The reason for the divergent results regarding the sustained drug release can be explained by different properties of the drug and the multilayer behavior under various temperature and environment conditions. In the present study, the challenge of controlling drug release was approached by the creative synthesis of TC/anionic  $\beta$ -CD. The idea here was to develop an antimicrobial coating capable of preventing infection; therefore, it is important to mention that a TC/anionic  $\beta$ -CD release under neutral pH demonstrated a discrete burst within the first 24 h, with a significant and continuous drug release over an extended period of time up to 15 days. By contrast, an expressive release of TC/anionic  $\beta$ -CD from [PAA/PLL]<sub>10</sub> coated Ti discs in acidic environment was observed at 24 h, which potentially mimics the acidity of inflammatory processes. One possible reason for the burst release of TC/anionic  $\beta$ -CD from the [PAA/PLL]<sub>10</sub> could be due to TC/anionic  $\beta$ -CD diffusing out of the superficial layer of the system, followed by a sustained release of TC/anionic  $\beta$ -CD complex due to strong interaction between this complex and the LbL coating. The high temperature and acidic pH cause film destabilization and disassembly by changing polyelectrolyte conformation and allowing

patterned drug diffusion through the multilayered LbL coating. We have previously demonstrated that the [PAA/PLL]<sub>10</sub> coating undergoes structural changes at a temperature of 37 °C in a wet environment (de Avila E.D. et al., 2019). It has been suggested that the polyelectrolyte multilayer conformation in the LbL coating is changed due to dehydration under high temperature. Further, a possible interference of pH on [PAA/PLL]<sub>10</sub> structure can explain the high values of drug released at acidic conditions (de Avila E.D. et al., 2019). Interestingly, comparable results were obtained to [PAA/PLL]<sub>10</sub>/TC/anionic  $\beta$ -CD coated Ti discs upon immersion in MH solution. However, MH culture medium discloses a pH value of 7.2, i.e., similar to the PBS (7.4), which means that other factors are also contributing to the drug diffusion through the [PAA/PLL]<sub>10</sub>. It has been already known that some culture media indicated for testing of bacterial susceptibility can have a profound influence on the results obtained. This can be explained by the largely to the ionic environment. The low concentration of calcium and magnesium present in the MH culture medium have also been observed to inhibit the antibacterial activity of tetracyclines against *Pseudomonas aeruginosa*, for example (Beggs & Andrews, 1976; Reller, Schoenknecht, Kenny, & Sherris., 1974). The literature has reported the nonspecific ionic strength-dependent effect in which the salt concentrations resulted in higher MICs for several bacteria species tested. This outcome means that salts present in the medium might contribute to increase its ionic strength, which in turn has a profound effect on the drug release from the coating.

Fig. 7 shows the TC original fluorescence from both [PAA/PLL]<sub>10</sub>/TC and [PAA/PLL]<sub>10</sub>/TC/anionic  $\beta$ -CD coating Ti discs before proceeding

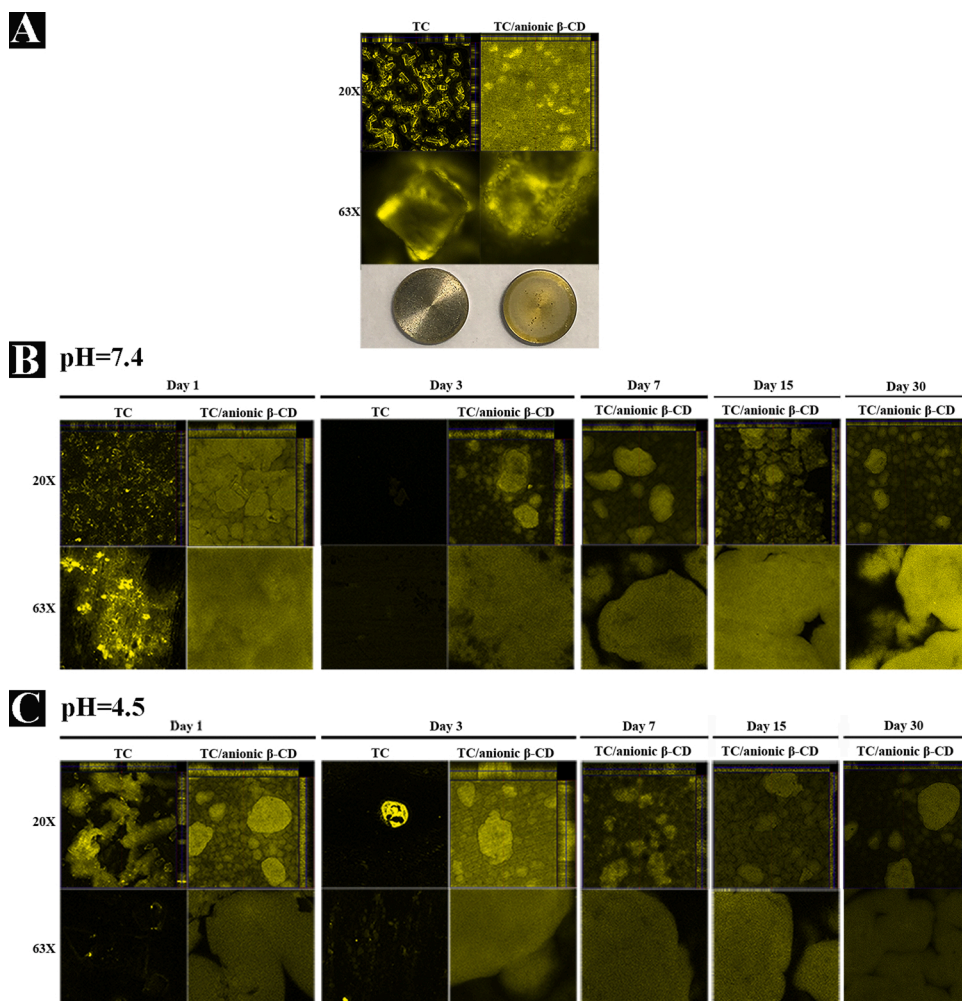


**Fig. 7.** (A) Tetracycline fluorescence intensity from both [PAA/PLL]<sub>10</sub>/TC and [PAA/PLL]<sub>10</sub>/TC/anionic  $\beta$ -CD coating Ti discs, before immersion steps. (B) Qualitative images of TC fluorescence intensity from both [PAA/PLL]<sub>10</sub>/TC and [PAA/PLL]<sub>10</sub>/TC/anionic  $\beta$ -CD coating Ti discs immersed in neutral solution, pH (pH = 7.4), in different time points. (C) Qualitative images of TC fluorescence intensity from both [PAA/PLL]<sub>10</sub>/TC and [PAA/PLL]<sub>10</sub>/TC/anionic  $\beta$ -CD coating Ti discs immersed in acidic solution, pH (pH = 4.5), in different time points.



with immersion solutions. We additionally acquired CLSM images (Figs. 7-A) to confirm the effectiveness of the interaction between TC/anionic  $\beta$ -CD and [PAA/PLL]<sub>10</sub> by TC autofluorescence. Image analyses revealed apparent coverage of the [PAA/PLL]<sub>10</sub> structure loaded with TC upon immersion under acidic and neutral solutions, with increased fluorescent signal for TC/anionic  $\beta$ -CD compared with only TC. Remarkably, LbL coatings loaded with TC showed minimal fluorescent signal from 3 days onward. In contrast, loading with TC/anionic  $\beta$ -CD clearly showed fluorescent signal even up to 30 days of incubation, independent on the pH of the incubation medium. Consistent with HPLC data, density of the TC/anionic  $\beta$ -CD fluorescence was significantly enhanced on [PAA/PLL]<sub>10</sub> coating Ti discs when in neutral pH (Fig. 7-B) compared with acidic pH (Fig. 7-C). This indicates that the degree of acidity might facilitate TC/anionic  $\beta$ -CD retention or its release from the LbL coating translated as highest or lowest fluorescence intensity, respectively.

### 3.5. [PAA/PLL]<sub>10</sub>/TC/anionic $\beta$ -CD antimicrobial activity against *S. Aureus*

Local drug administration is a straightforward approach to limit occurrence of antibiotic resistance, still providing sufficient antibacterial activity at a specific target and decreasing systemic toxicity (Chellat, Raguz, & Riedl, 2016). Here, TC loaded into the LbL coatings was increased from the MBC data to extend the amount of TC available in the environment over time. The sustained release of TC from LbL coatings depends on the total amount of TC and release kinetics, the latter related to the electrostatic interactions with the LbL coating. The antimicrobial activity of [PAA/PLL]<sub>10</sub>/TC/anionic  $\beta$ -CD coating on Ti discs was

evaluated using standard colony-forming unit (CFU) analysis. We selected *S. aureus* as it is the most common bacterial species associated with biofilms formed on medical devices and widely recognized as a major source of healthcare-associated infections (Gotz, 2002; von Eiff, Jansen, Kohnen, & Becker, 2005). After 48 h of incubation, the number of colonies formed on each agar plate was counted, and data demonstrated a strong antimicrobial effect of the [PAA/PLL]<sub>10</sub>/TC/anionic  $\beta$ -CD coating with more than 5 log reduction of bacterial growth in comparison to the uncoated Ti discs (Fig. 8A). Similar antimicrobial effect was also obtained from [PAA/PLL]<sub>10</sub>/TC group. However, amphiphile anionic  $\beta$ -CD complex was clearly responsible for retaining tetracycline and controlling its release from the LbL coating, over time. Quantitative data from HPLC analyses confirmed a controlled release of TC/anionic  $\beta$ -CD higher than the MBC over a period of 7–15 days. Interestingly, the antibacterial activity of TC/anionic  $\beta$ -CD retained into the [PAA/PLL]<sub>10</sub> system remained even up to 30 days of incubation under acidic and neutral pH, with 2.8 log reduction of *S. aureus* compared with uncoated Ti discs.

Clinical trials show that we cannot afford to rely solely on local administration of antimicrobial drugs for patients undergoing surgical implantation (Darouiche, 2003). However, local antibiotic approaches take the advantage of providing higher local concentrations of drugs on and/or around the implant and provide more protection against implant-associated infection. Our effective drug releasing LbL coatings point toward applicability for Ti implants capable to release an appropriate dose of TC/anionic  $\beta$ -CD and increased duration of antimicrobial coverage. However, additional microbiology experiments must be done to confirm the potential effect of our LbL coating against representative polymicrobial communities from PDS.

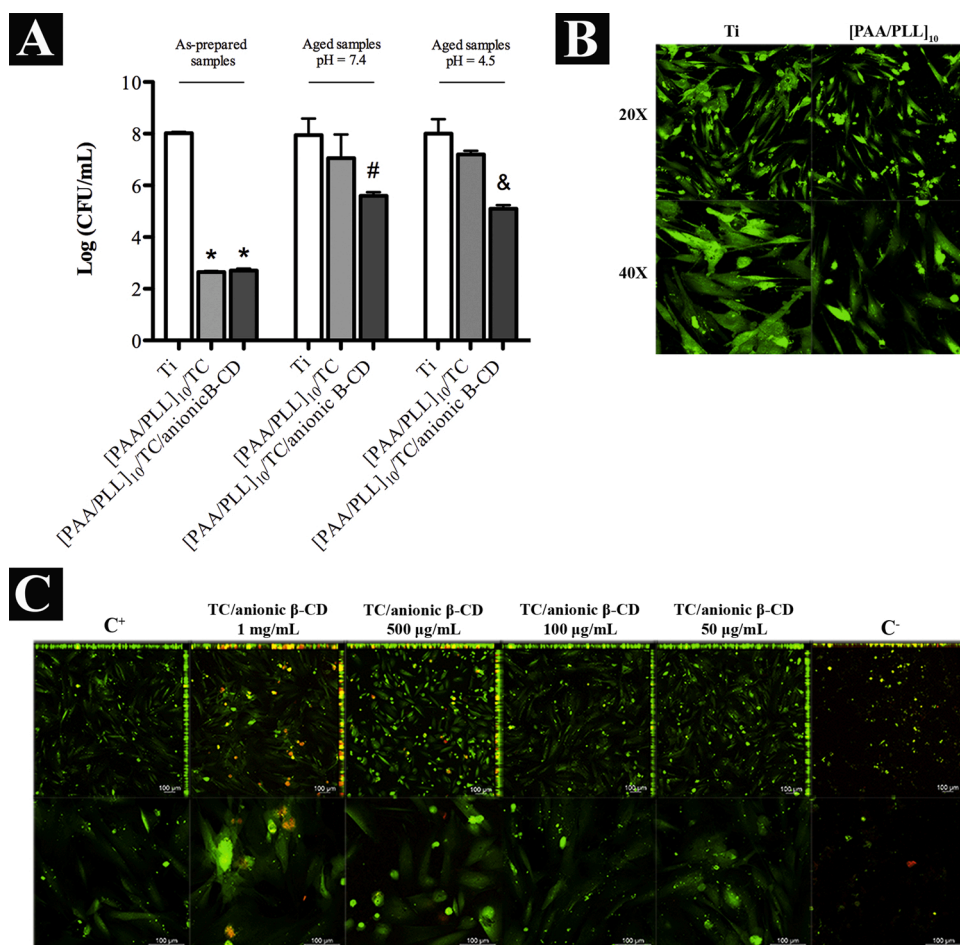


**Fig. 8.** (A) Quantitative measurement of log CFU/mL showing *S. aureus* accumulation on uncoated Ti (white bar, Ti), [PAA/PLL]<sub>10</sub>/TC (light gray bar) and [PAA/PLL]<sub>10</sub>/TC/anionic  $\beta$ -CD coating Ti discs (dark gray bar) on fresh samples (as-prepared), and aged samples after 30 days of immersion in both neutral (pH = 7.4) and acidic (pH = 4.5) conditions. Data are shown as the mean  $\pm$  standard deviation. Statistically significant differences are indicated as: \*, #, & p < 0.0001 vs Ti control. (B) Effect of [PAA/PLL]<sub>10</sub> coating Ti discs on HGF cell viability at 24 h of culture via live (CFSE)/dead (PI) analysis (green for live cells, red for dead cells). (C) Effect of TC/anionic  $\beta$ -CD concentrations on HGF cell viability at 24 h of culture via live (CFSE)/dead (PI) analysis (green for live cells, red for dead cells).

### 3.6. Cytocompatibility of [PAA/PLL]<sub>10</sub> coating

PDs comprise a metallic post attached to the bone that extends outward through the skin to connect to an external prosthesis. Therefore, fibroblasts and keratinocytes are the major cell types involved in the inflammatory response in the cutaneous repair/regeneration process. Previously, we determined the cytocompatibility of the engineered LbL system on viability of HaCaT immortalized human keratinocytes cell. Further experiments were performed to confirm the non-cytotoxicity effect of a high TC concentration of 500 µg/mL on mammalian cells after 72 h of incubation (de Avila E.D. et al., 2019). Herein, we used confocal microscopy to evaluate whether [PAA/PLL]<sub>10</sub> coated Ti discs affect viability and spreading of human gingival fibroblast. Additionally, to eliminate the biosafety concerns associated with TC/anionic β-CD concentration released from [PAA/PLL]<sub>10</sub> coating Ti discs, different drug concentrations were used for HGF cell cultures. Carboxyfluorescein succinimidyl ester (CFSE) is a non-fluorescent dye that diffuses across cell membranes to be cleaved within the cell by intracellular esterases. The cleaved CFSE is highly fluorescent and covalently binds to protein amine groups within the cell, identifying live cells capable of proliferating (Wang, D. X., Liu, Fang, & Tan, 2005). Qualitative images demonstrated that [PAA/PLL]<sub>10</sub> coated Ti discs did not affect the proliferation and spreading of metabolically active cells in vitro, revealing similar fluorescence and spreading of the HGF cells on [PAA/PLL]<sub>10</sub> coating and Ti control surfaces (Fig. 8B). Comparably, *in vitro* cell-based cytotoxicity assay revealed that none of the concentrations assessed affected HGF cell morphology and viability, over a sufficient period to measure the hazard potential (Fig. 8C). The images clearly show live cells for all TC/anionic β-CD concentrations tested when in comparison to the positive control (C<sup>+</sup>), as represented by green fluorescence. By contrast, the negative control (C<sup>-</sup>) directly affected the propagation of HGF cells and caused its death. The loss of membrane integrity was determined by red fluorescence.

### 4. Conclusion and future perspective

The critical medical consequences and the sequel of infection associated with percutaneous implants devices underscore the importance of creating strategies for prevention and treatment, impervious to antibiotic resistance. In this work, we improved the drug loading and release for LbL coatings by creating a complex between hydrophilic tetracycline and an amphiphilic anionic β-CD. The strong interaction between tetracycline - anionic β-CD, and effective loading of the complex in [PAA/PLL]<sub>10</sub> enabled tetracycline retention within the LbL coatings for prolonged time, regardless of medium pH. The need for amphiphile anionic beta cyclodextrin (β-CD) complexes to retain tetracycline and control its release from [PAA/PLL]<sub>10</sub> was clearly demonstrated when [PAA/PLL]<sub>10</sub>/TC/anionic β-CD was compared with its counterpart group ([PAA/PLL]<sub>10</sub>/TC). Microscopy images using a high numerical aperture lens displayed no fluorescence intensity from [PAA/PLL]<sub>10</sub>/TC group after 3 days incubation in both neutral and acidic mediums. The effective [PAA/PLL]<sub>10</sub>/TC/anionic β-CD coating on Ti surface showed to be readily tunable to different physiological scenarios, with a controlled release of TC at different pH conditions, but with a significant and convenient higher release under acidic environment, simulating inflammatory process characteristics. Importantly, TC/anionic β-CD concentration released from [PAA/PLL]<sub>10</sub> coating did not affect HGF cells viability. Antibacterial effect of [PAA/PLL]<sub>10</sub>/TC/anionic β-CD was confirmed against *S. aureus* ATCC 25,923, with more than 5 log reduction of bacterial growth remaining after 48 h of incubation days. An extended effect in *S. aureus* reducing on [PAA/PLL]<sub>10</sub>/TC/anionic β-CD discs in comparison with uncoated Ti discs was maintained even up to 30 days incubation, indicating a remained activity of TC/anionic β-CD retained into the [PAA/PLL]<sub>10</sub> system. Further microbiology experiments are required to confirm the potential effect of the LbL coating against a representative polymicrobial community from PDs. In

addition, *in vivo* experiments will provide new insights regarding the LbL coating role on inflammatory signaling pathways to facilitate the advancement of this technology for biomedical applications. Taken together, our results demonstrate the potential of this novel drug-releasing coating for the engineering of antimicrobial coatings in a facile manner.

### 5. Author contributions

Beatriz S. Verza: Formal analysis, investigation, methodology and data interpretation.

Jeroen van den Beucken: Conceptualization, data interpretation, review & editing and resource.

João V. Brandt: Investigation, methodology, data interpretation and review & editing.

Miguel Jafelici Junior: Conceptualization, methodology and resource.

Valentim A. R. Barão: Conceptualization, methodology, data interpretation and review & editing.

Rodolfo D. Piazza: Investigation, methodology, data interpretation and review & editing.

Oya Tagit: Investigation, methodology and data interpretation.

Denise M. P. Spolidorio: Conceptualization, methodology and resource.

Carlos Eduardo Vergani: Methodology and resource.

Erica D. de Avila: Conceptualization, funding acquisition; investigation; methodology; supervision; visualization; roles/writing - original draft.

### Acknowledgements

Erica Dorigatti de Avila was supported by The São Paulo Research Foundation (FAPESP) grant # 2015/03567-7. Beatriz Severino Verza was supported by The São Paulo Research Foundation (FAPESP) grant # 2018/19345-1.

### Appendix A. Supplementary data

Supplementary material related to this article can be found, in the online version, at doi:<https://doi.org/10.1016/j.carbpol.2020.117604>.

### References

- Abdallah, M. N., Badran, Z., Ciobanu, O., Hamdan, N., & Tamimi, F. (2017). Strategies for optimizing the Soft tissue seal around osseointegrated implants. *Advanced Healthcare Materials*, 6(20).
- Affeld, K., Grosshauser, J., Goubergrits, L., & Kertzsch, U. (2012). Percutaneous devices: A review of applications, problems and possible solutions. *Expert Review of Medical Devices*, 9(4), 389–399.
- Archontaki, H. A., Vertzoni, M. V., & Athanassiou-Malaki, M. H. (2002). Study on the inclusion complexes of bromazepam with beta- and beta-hydroxypropyl-cyclodextrins. *Journal of Pharmaceutical and Biomedical Analysis*, 28(3-4), 761–769.
- Arima, H., Miyaji, T., Irie, T., Hirayama, F., & Uekama, K. (1998). Enhancing effect of hydroxypropyl-beta-cyclodextrin on cutaneous penetration and activation of ethyl 4-biphenyl acetate in hairless mouse skin. *European Journal of Pharmaceutical Sciences*, 6(1), 53–59.
- Arima, H., Yunomae, K., Miyake, K., Irie, T., Hirayama, F., & Uekama, K. (2001). Comparative studies of the enhancing effects of cyclodextrins on the solubility and oral bioavailability of tacrolimus in rats. *Journal of Pharmaceutical Science*, 90(6), 690–701.
- Beggs, W. H., & Andrews, F. A. (1976). Role of ionic strength in salt antagonism of aminoglycoside action on *Escherichia coli* and *Pseudomonas aeruginosa*. *The Southern African Journal of Epidemiology & Infection: Official Journal of the Sexually Transmitted Diseases, Infectious Diseases and Epidemiological Societies of Southern Africa*, 134(5), 500–504.
- Beline, T., da Silva, J. H. D., Matos, A. O., Azevedo Neto, N. F., de Almeida, A. B., Nociti Junior, F. H., et al. (2019). Tailoring the synthesis of tantalum-based thin films for biomedical application: Characterization and biological response. *Materials Science & Engineering C, Materials for Biological Applications*, 101, 111–119.
- Boehler, C., Kleber, C., Martini, N., Xie, Y., Dryg, I., Stieglitz, T., et al. (2017). Actively controlled release of Dexamethasone from neural microelectrodes in a chronic *in vivo* study. *Biomaterials*, 129, 176–187.

- Campoccia, D., Montanaro, L., & Arciola, C. R. (2006). The significance of infection related to orthopedic devices and issues of antibiotic resistance. *Biomaterials*, 27(11), 2331–2339.
- Cha, J. K., Lee, J. S., & Kim, C. S. (2019). Surgical therapy of peri-implantitis with local minocycline: A 6-Month randomized controlled clinical trial. *Journal of Dental Research*, 98(3), 288–295.
- Chellat, M. F., Raguz, L., & Riedl, R. (2016). Targeting antibiotic resistance. *Angewandte Chemie International Edition in English*, 55(23), 6600–6626.
- Costa, R. C., Souza, J. G. S., Cordeiro, J. M., Bertolini, M., de Avila, E. D., Landers, R., et al. (2020). Synthesis of bioactive glass-based coating by plasma electrolytic oxidation: Untangling a new deposition pathway toward titanium implant surfaces. *Journal of Colloid and Interface Science*, 579, 680–698.
- Croitoru, C., Roata, I. C., Pascu, A., & Stanciu, E. M. (2020). Diffusion and controlled release in physically crosslinked poly (Vinyl alcohol)/Iota-Carrageenan hydrogel blends. *Polymers*, 12(7), 1544.
- Darouiche, R. O. (2003). Antimicrobial approaches for preventing infections associated with surgical implants. *Clinical Infections Diseases*, 36(10), 1284–1289.
- de Avila, E. D., van Oirschot, B. A., & van den Beucken, J. (2020). Biomaterial-based possibilities for managing peri-implantitis. *Journal of Periodontal Research*, 55(2), 165–173.
- de Avila, E. D., C. A., Tagit, O., Krom, B. P., Löwik, D., van Well, A. A., Bannenberg, L. J., et al. (2019). Anti-bacterial efficacy via drug-delivery system from layer-by-layer coating for percutaneous dental implant components. *Applied Surface Science*, 488, 194–204.
- Deng, H., Liu, J., Zhao, X., Zhang, Y., Liu, J., Xu, S., et al. (2014). PEG-b-PCL copolymer micelles with the ability of pH-controlled negative-to-positive charge reversal for intracellular delivery of doxorubicin. *Biomacromolecules*, 15(11), 4281–4292.
- Dini, C., Nagay, B. E., Cordeiro, J. M., da Cruz, N. C., Rangel, E. C., Ricomini-Filho, A. P., et al. (2020). UV-photofunctionalization of a biomimetic coating for dental implants application. *Materials Science & Engineering C, Materials for Biological Applications*, 110, Article 110657.
- Donath, E., Sukhorukov, G. B., Caruso, F., Davis, S. A., & Mohwald, H. (1998). Novel hollow polymer shells by colloid-templated assembly of polyelectrolytes. *Angewandte Chemie International Edition in English*, 37(16), 2201–2205.
- Drago, L., Boot, W., Dimas, K., Malizos, K., Hansch, G. M., Stuyck, J., et al. (2014). Does implant coating with antibiotic-loaded hydrogel reduce bacterial colonization and biofilm formation in vitro? *Clinical Orthopaedics and Related Research*, 472(11), 3311–3323.
- Gomez-Galvan, F., Perez-Alvarez, L., Matas, J., Alvarez-Bautista, A., Poejo, J., Duarte, C. M., et al. (2016). Preparation and characterization of soluble branched ionic beta-cyclodextrins and their inclusion complexes with triclosan. *Carbohydrate Polymers*, 142, 149–157.
- Gotz, F. (2002). Staphylococcus and biofilms. *Molecular Microbiology*, 43(6), 1367–1378.
- Groeger, S. E., & Meyle, J. (2015). Epithelial barrier and oral bacterial infection. *Periodontology 2000*, 69(1), 46–67.
- Han, J., & Ulevitch, R. J. (2005). Limiting inflammatory responses during activation of innate immunity. *Nature Immunology*, 6(12), 1198–1205.
- Han, Y. W., & Wang, X. (2013). Mobile microbiome: Oral bacteria in extra-oral infections and inflammation. *Journal of Dental Research*, 92(6), 485–491.
- Hasanzadeh, M., Sadeghi, S., Bageri, L., Mokhtarzadeh, A., Karimzadeh, A., Shadjou, N., et al. (2016). Poly-dopamine-beta-cyclodextrin: A novel nanobiopolymer towards sensing of some amino acids at physiological pH. *Materials Science & Engineering C, Materials for Biological Applications*, 69, 343–357.
- Hollenbeak, C. S., & Schilling, A. L. (2018). The attributable cost of catheter-associated urinary tract infections in the United States: A systematic review. *American Journal of Infection Control*, 46(7), 751–757.
- Jeong, J., Song, W., Cooper, W. J., Jung, J., & Greaves, J. (2010). Degradation of tetracycline antibiotics: Mechanisms and kinetic studies for advanced oxidation/reduction processes. *Chemosphere*, 78(5), 533–540.
- Jepsen, K., & Jepsen, S. (2016). Antibiotics/antimicrobials: Systemic and local administration in the therapy of mild to moderately advanced periodontitis. *Periodontology 2000*, 71(1), 82–112.
- Jia, Y., & Li, J. (2019). Molecular assemblies of biomimetic microcapsules. *Langmuir*, 35(26), 8557–8564.
- Kane, S. F. (2017). The effects of oral health on systemic health. *General Dentistry*, 65(6), 30–34.
- Kang, S., Park, G. H., Kim, S., Kim, J., Choi, Y., Huang, Y., et al. (2019). In vitro and in vivo antimicrobial activity of antibiotic-conjugated carriers with rapid pH-Responsive release kinetics. *Advanced Healthcare Materials*, 8(14), Article e1900247.
- Koldsland, O. C., Scheie, A. A., & Aass, A. M. (2010). Prevalence of peri-implantitis related to severity of the disease with different degrees of bone loss. *Journal of Periodontology*, 81(2), 231–238.
- Lade, H., Park, J. H., Chung, S. H., Kim, I. H., Kim, J. M., Joo, H. S., et al. (2019). Biofilm formation by Staphylococcus aureus clinical isolates is differentially affected by glucose and sodium chloride supplemented culture media. *Journal of Clinical Medicine*, 8(11), 1853.
- Laza-Knoerr, A. L., Gref, R., & Couvreur, P. (2010). Cyclodextrins for drug delivery. *Journal of Drug Targeting*, 18(9), 645–656.
- Li, X., Kolltveit, K. M., Tronstad, L., & Olsen, I. (2000). Systemic diseases caused by oral infection. *Clinical Microbiology Reviews*, 13(4), 547–558.
- Mahan, J., Seligson, D., Henry, S. L., Hynes, P., & Dobbins, J. (1991). Factors in pin tract infections. *Orthopedics*, 14(3), 305–308.
- Nagay, B. E., Dini, C., Cordeiro, J. M., Ricomini-Filho, A. P., de Avila, E. D., Rangel, E. C., et al. (2019). Visible-light-Induced photocatalytic and antibacterial activity of TiO2 codoped with nitrogen and Bismuth: New perspectives to control implant-biofilm-Related diseases. *ACS Applied Materials & Interfaces*, 11(20), 18186–18202.
- Paczkowska, M., Szymanowska-Powalowska, D., Mizera, M., Siakowska, D., Blaszczyk, W., Piotrowska-Kempisty, H., et al. (2019). Cyclodextrins as multifunctional excipients: Influence of inclusion into beta-cyclodextrin on physicochemical and biological properties of tebipenem pivoxil. *PLoS One*, 14(1), Article e0210694.
- Pavia, D. L., Lampman, G. M., & Kriz, G. S. (2001). *Infrared spectroscopy Introduction to spectroscopy: A guide for student of organic chemistry* (3 ed., p. 579). South Melbourne: Thomson Learning.
- Peramo, A., & Marcelo, C. L. (2010). Bioengineering the skin-implant interface: The use of regenerative therapies in implanted devices. *Annals of Biomedical Engineering*, 38(6), 2013–2031.
- Percival, S. L., Suleman, L., Vuotto, C., & Donelli, G. (2015). Healthcare-associated infections, medical devices and biofilms: Risk, tolerance and control. *Journal of Medical Microbiology*, 64(Pt 4), 323–334.
- Perez-Alvarez, L., Matas, J., Gomez-Galvan, F., Ruiz-Rubio, L., Leon, L. M., & Vilas-Vilela, J. L. (2017). Branched and ionic beta-Cyclodextrins multilayer assembling onto polyacrylonitrile membranes for removal and controlled release of triclosan. *Carbohydrate Polymers*, 156, 143–151.
- Puckett, S. D., Lee, P. P., Ciombor, D. M., Aaron, R. K., & Webster, T. J. (2010). Nanotextured titanium surfaces for enhancing skin growth on transcutaneous osseointegrated devices. *Acta Biomaterialia*, 6(6), 2352–2362.
- Radu, C. D., Parteni, O., & Ochiuz, L. (2016). Applications of cyclodextrins in medical textiles - review. *Journal of Controlled Release*, 224, 146–157.
- Regassa, L. B., Novick, R. P., & Betley, M. J. (1992). Glucose and nonmaintained pH decrease expression of the accessory gene regulator (agr) in Staphylococcus aureus. *Infection and Immunity*, 60(8), 3381–3388.
- Reinbold, J., Hierlemann, T., Ulrich, L., Uhde, A. K., Muller, I., Weindl, T., et al. (2017). Biodegradable rifampicin-releasing coating of surgical meshes for the prevention of bacterial infections. *Drug Design, Development and Therapy*, 11, 2753–2762.
- Reller, L. B., Schoenknecht, F. D., Kenny, M. A., & Sherris, J. C. (1974). Antibiotic susceptibility testing of Pseudomonas aeruginosa: Selection of a control strain and criteria for magnesium and calcium content in media. *The Southern African Journal of Epidemiology & Infection: Official Journal of the Sexually Transmitted Diseases, Infectious Diseases and Epidemiological Societies of Southern Africa*, 130, 454–463.
- Santos, C., Ribeiro, A. C. F., & Esteso, M. A. (2019). Drug delivery systems: Study of inclusion complex formation between Methylxanthines and cyclodextrins and their thermodynamic and transport properties. *Biomolecules*, 9(5), 1–21.
- Scannapieco, F. A., & Mylotte, J. M. (1996). Relationships between periodontal disease and bacterial pneumonia. *Journal of Periodontology*, 67(10 Suppl), 1114–1122.
- Souza, J. G. S., Bertolini, M., Costa, R. C., Cordeiro, J. M., Nagay, B. E., de Almeida, A. B., et al. (2020). Targeting pathogenic biofilms: Newly developed superhydrophobic coating favors a host-compatible microbial profile on the titanium surface. *ACS Applied Materials & Interfaces*, 12(9), 10118–10129.
- Stacy, A., Everett, J., Jorth, P., Trivedi, U., Rumbaugh, K. P., & Whiteley, M. (2014). Bacterial fight-and-flight responses enhance virulence in a polymicrobial infection. *Proceedings of the National Academy of Sciences*, 111(21), 7819–7824.
- Stadler, B., Chandrawati, R., Goldie, K., & Caruso, F. (2009). Capsosomes: Subcompartmentalizing polyelectrolyte capsules using liposomes. *Langmuir*, 25(12), 6725–6732.
- Stone, M. R. L., Butler, M. S., Phetsang, W., Cooper, M. A., & Blaskovich, M. A. T. (2018). Fluorescent antibiotics: New research tools to fight antibiotic resistance. *Trends in Biotechnology*, 36(5), 523–536.
- Tiwari, G., Tiwari, R., & Rai, A. K. (2010). Cyclodextrins in delivery systems: Applications. *Journal of Pharmacy & Biomedical Sciences*, 2(2), 72–79.
- Tsiskandylakis, G., Berlin, O., & Branemark, R. (2014). Implant survival, adverse events, and bone remodeling of osseointegrated percutaneous implants for transhumeral amputees. *Clinical Orthopaedics and Related Research*, 472(10), 2947–2956.
- van den Beucken, J. J., Vos, M. R., Thune, P. C., Hayakawa, T., Fukushima, T., Okahata, Y., et al. (2006). Fabrication, characterization, and biological assessment of multilayered DNA-coatings for biomaterial purposes. *Biomaterials*, 27(5), 691–701.
- Varan, G., Varan, C., Erdogar, N., Hincal, A. A., & Bilensou, E. (2017). Amphiphilic cyclodextrin nanoparticles. *International Journal of Pharmaceutics*, 531(2), 457–469.
- von Eiff, C., Jansen, B., Kohnen, W., & Becker, K. (2005). Infections associated with medical devices: Pathogenesis, management and prophylaxis. *Drugs*, 65(2), 179–214.
- Wang, X., D. X., Liu, L. H., Fang, Y. Q., & Tan, Q. (2005). Carboxyfluorescein diacetate succinimidyl ester fluorescent dye for cell labeling. *Acta Biochimica et Biophysica Sinica*, 37(6), 379–385.
- Xu, Y., Larsen, L. H., Lorenzen, J., Hall-Stoodley, L., Kikhney, J., Moter, A., et al. (2017). Microbiological diagnosis of device-related biofilm infections. *APMIS*, 125(4), 289–303.
- Yin, L., Xu, S., Feng, Z., Deng, H., Zhang, J., Gao, H., et al. (2017). Supramolecular hydrogel based on high-solid-content mPCL nanoparticles and cyclodextrins for local and sustained drug delivery. *Biomaterials Science*, 5(4), 698–706.
- Yue, C., Zhao, B., Ren, Y., Kuijter, R., van der Mei, H. C., Busscher, H. J., et al. (2015). The implant infection paradox: Why do some succeed when others fail? Opinion and discussion paper. *European Cells & Materials*, 29, 303–310.
- Zimlichman, E., Henderson, D., Tamir, O., Franz, C., Song, P., Yamin, C. K., et al. (2013). Health care-associated infections: A meta-analysis of costs and financial impact on the US health care system. *JAMA Internal Medicine*, 173(22), 2039–2046.